Revisiting the Humidity Ramp Protocol for Assessing Human Heat Tolerance Limits

Fèlix Faming Wang[a,b,*], Yi Xu[b], Haojian Wang[b], Min Cui[b], Xue Hou[b], Boan Wei[b], Xiong Shen[a]

[a] One Health Research Group (OHRG), School of Environmental Science and Engineering, Tianjin University, Tianjin 300354, China

[b] Center for Molecular Biology and Non-Communicable Diseases Research, School of Safety Science and Engineering, Xi'an University of Science and Technology, Xi'an 710054, China

*Correspondence should be addressed to F.F.W. (famingwang@tju.edu.cn)

Word count: 7,175 words (New & Noteworthy, figures, tables & references excluded)

Running head: Revisiting humidity ramp protocols

***Correspondence address**

Prof. dr. Fèlix Faming Wang

One Health Research Group

School of Environmental Science and Engineering

Tianjin University Peiyang Park Campus

No.135 Yaguan Road, Haihe Education Park, Tianjin 300354

China

Tel.: +86 13430811617

Note: This manuscript was initially posted as a preprint: Faming Wang, Yi Xu, Haojian Wang, Min Cui, Xue Hou, & Boan Wei (2025). Revisiting humidity ramp protocols for assessing human heat tolerance. *bioRxiv*, 2025.11.09.686670, doi:10.1101/2025.11.09.686670. The corresponding author (Fèlix Faming Wang) previously published under the name Faming Wang.

Abstract (249 words)

Background: Humidity ramp protocols are widely used to assess human heat tolerance limits, but the impact of ramp temporal structure (e.g., step duration) on estimated critical environmental limits (CELs) remains unclear. This study integrated theoretical modeling and empirical testing to assess these effects on apparent core temperature (T_{cr}) inflection points.

Methods: A first-order thermal model described T_{cr} dynamics during stepwise humidity changes at fixed dry-bulb temperature (T_{db}), with analytical solutions for increments of duration Δt and sensitivity analyses across relevant time constants (τ). Twenty-six healthy young adults (14 males, 12 females) completed randomized trials at T_{db}=42 °C: (1) *slow-ramp* (4-hour equilibration at 40% RH, then +6% RH/hour for 2 hours followed by +3% RH/hour; RH range: 40–61%) and (2) *aggressive-ramp* (30 min equilibration, then +2% RH every 5 min; RH range: 28–88%). Rectal and skin temperatures, heart rate, and perceptual ratings were monitored continuously.

Results: When $\Delta t/\tau \ll 1$, thermal disequilibrium accelerated T_{cr} rises, yielding prematurely low CELs; dwell times ≥ 60 min/step permitted near-equilibrium and higher thresholds. Aggressive-ramp CELs were significantly lower than slow-ramp (males: 29.9±1.6 °C vs. 33.4±0.5 °C; females: 30.3±0.9 °C vs. 33.8±0.5 °C), with downward shifts of 3.4±1.9 °C and 3.5±0.9 °C, respectively.

Conclusion: Rapid humidity increments systematically underestimate heat tolerance due to thermal lag. Accurate CEL determination requires prolonged stable exposures (gold standard) or slow ramps ensuring sufficient equilibration ($\Delta t \geq 60$ min/step). Our findings reveal a core limitation of aggressive-ramp protocols and offer a framework for improved assessment of human environmental compensability.

Keywords: humidity-ramp; core temperature inflection point; critical environmental limit; heat tolerance; prolonged exposure

NEW & NOTEWORTHY (75 words)

This study reveals how ramp temporal structure affects heat tolerance assessment. Rapid humidity increments in aggressive-ramp protocols cause premature underestimation of critical environmental limits (CELs) due to thermal disequilibrium. In contrast, prolonged dwell times (≥ 60 min/step) in slow ramps allow near-equilibrium conditions, resulting in higher and more accurate CELs. These findings emphasize the importance of equilibration time in defining heat tolerance and provide a more reliable approach for assessing heat stress in extreme environments.

1 | Introduction

As global temperatures rise and extreme heatwaves become increasingly frequent, intense, and prolonged (1), understanding the physiological limits of human heat tolerance has never been more crucial (2–5). A central challenge is defining the critical environmental limits (CELs) beyond which the human body can no longer maintain thermal equilibrium. CELs are commonly quantified using wet-bulb temperature (T_w), which combines dry-bulb temperature (T_{db}) and humidity to assess heat stress. Crossing these limits results in uncompensable heat stress, characterized by a rapid elevation in core temperature (T_{cr}) and an increased risk of heat-related illnesses (6, 7).

A widely used experimental approach to identify CELs is the *humidity ramp protocol* (also known as the *thermal-step* or *core temperature inflection-point* protocol), first introduced by Belding and Kamon (8). In its classical form, this method progressively increases relative humidity in fixed increments—typically 1 mm Hg every 10 minutes—following an initial 60-minute core temperature stabilization period at a constant T_{db} and low humidity (9). It should be noted that humidity adjustments in the test chamber typically reach their new target within a few minutes (2–5 min), meaning that these 'ramps' are implemented as stepwise increments rather than truly continuous changes. The point at which T_{cr} rises uncontrollably is interpreted as the delineation from compensable to uncompensable heat stress. Recent studies have adopted modified versions of this approach to determine CELs across populations and environmental conditions (10–14). However, reported humidity-ramp protocols differ substantially in their initial stabilization durations, step magnitudes, and ramp rates. For instance, some studies implemented a 30-minute stabilization phase followed by either a 1 mm Hg increase in ambient water vapor pressure (p_{air}) or a 3% increase in relative humidity every 5 minutes (10–14), whereas others employed 1 °C increases in dry-bulb temperature or 1 mm Hg p_{air} increments every 10 minutes (8, 9). More recently, some studies (15, 16) adopted a 70-minute equilibration period, followed by 3% RH (approximately 1.85 mm Hg) increments every 10 minutes.

Despite broadly similar participant characteristics and testing protocols, reported CELs vary markedly, ranging from approximately 26 °C to 33 °C in young adults with metabolic rates of 1.3–1.5 Mets (10–16). This wide variability raises a fundamental methodological concern: does the arbitrary choice of ramp rate and step duration influence the accuracy of predicted CELs? Such variation is difficult to explain by participant factors alone, suggesting that methodological differences—particularly ramp dwell time—may have a substantial impact on the accuracy of predicted CELs.

Our recent work suggested that environments previously classified as uncompensable using humidity-ramp protocols were, in fact, fully compensable when evaluated using prolonged stable

exposure, the gold standard for assessing environmental uncompensability (17). This finding indicates that the humidity-ramp protocol may systematically predict uncompensable conditions that are, physiologically, still within compensable limits. While this highlights a significant source of potential bias, the mechanistic basis for this misclassification remains unclear, and explanations have often been attributed to inter-individual factors, such as ethnicity or heat-acclimatization status.

A central premise of the classical ramp approach is that the human thermoregulatory system reaches a new steady state after each stepwise increment in environmental humidity prior to the subsequent step change. In practice, however, the short dwell periods commonly employed (5–10 minutes) are frequently inadequate for full thermal equilibration, especially when heat storage is substantial and evaporative heat loss is limited. Prolonged stable-exposure studies have shown that core temperature stabilization can take up to 9–12 hours under extreme heat and humidity (18, 19). This finding prompts a fundamental question: does the characteristic inflection in core temperature (T_{cr}) mark the genuine onset of uncompensable heat stress, or does it primarily reflect a transient lag between the body's instantaneous thermal state and its continually shifting equilibrium?

To distinguish whether the inflection in core temperature (T_{cr}) signifies a genuine physiological threshold or arises as a methodological artifact, we tested the hypothesis that apparent CELs are predominantly governed by the duration of each humidity step. Specifically, we proposed that short dwell times preclude the establishment of thermal steady state, thereby inducing an early, artifactual elevation in T_{cr} that is frequently misinterpreted as the onset of uncompensable heat stress. To isolate this effect while controlling for inter-individual variability (including ethnicity and heat-acclimatization status), we varied the humidity-increase rate across a range of timescales under constant T_{db} using young adult cohorts. In parallel, we developed a first-order dynamic model to describe T_{cr} responses to humidity ramp. Together, the experimental and modeling evidence reveals how ramp-rate artifacts systematically bias estimates of CELs and provides evidence-based guidelines for designing physiologically valid humidity-ramp protocols.

2 | Methods

2.1 | Model derivation and assumptions

The temporal evolution of core temperature (T_{cr}) during progressive humidity changes was derived from the first principles of whole-body heat balance. The human body is modeled as a single, lumped thermal compartment that exchanges heat with the surrounding environment via convection, radiation,

and evaporation. At any time t, the rate of body heat storage equals the rate of metabolic heat production minus the combined dry (convective and radiative) and evaporative heat losses (20)

$$C\frac{dT_{cr}}{dt} = \dot{M} - \dot{W} + \dot{Q}_{res} - \dot{Q}_{skin} \qquad \text{Eq.(1)}$$

where, C is the effective whole-body heat capacity (J/°C); $\dot{M}$ is metabolic heat production rate (W); $\dot{W}$ is external mechanical work rate (Watt; $\dot{W}\approx 0$ watt under seated conditions); $\dot{Q}_{res}$ and $\dot{Q}_{skin}$ are respiratory and skin heat exchange rates (W), respectively.

The net heat loss through the skin surface can be expressed as the sum of convective, radiative, and evaporative fluxes (18)

$$\dot{Q}_{skin} = \dot{Q}_{conv} + \dot{Q}_{rad} + \dot{Q}_{evap} \qquad \text{Eq.(2)}$$

with $\dot{Q}_{conv} = h_c A_s (T_{sk} - T_a)$, $\dot{Q}_{rad} = h_r A_s (T_{sk} - T_r)$, and $\dot{Q}_{evap} = h_e A_s (p_{sk} - p_{air})$

where, h_c, h_r, and h_e are the convective, radiative, and evaporative heat transfer coefficients (W/m²/°C), respectively; A_s is body surface area (m^2); T_{sk} is mean skin temperature (°C); T_a and T_r are ambient air (dry-bulb) and mean radiant temperatures(°C), respectively; p_{sk} is the water vapor pressures at the skin surface (Pa).

Under the classical humidity ramp experimental conditions—where air temperature is held constant and relative humidity progressively increases—metabolic heat production ($\dot{M}$) and respiratory heat exchange ($\dot{Q}_{res}$) can be treated as approximately constant. Consequently, variations in total heat loss are primarily governed by humidity-dependent changes in the potential for sweat evaporation (21, 22). To obtain a tractable representation of the system's transient thermal response, the net heat exchange was linearized around the steady-state operating point:

$$\dot{M} - \dot{W} + \dot{Q}_{res} - \dot{Q}_{skin} \approx -k[T_{cr}(t) - T_{cr,eq}(t)] \qquad \text{Eq.(3)}$$

where, $T_{cr,eq}$ is the equilibrium core temperature that would be achieved if the environment were held constant indefinitely (°C). k is an effective whole-body heat transfer coefficient (W/°C)—the lumped sum of convective, radiative, and evaporative heat conductances, modulated by physiological control of skin blood flow and sweating. Mathematically, k represents how efficiently excess body heat is dissipated when T_{cr} exceeds equilibrium, which is read as:

$$k = -\left.\frac{d(\dot{M} - \dot{Q}_{loss})}{dT_{cr}}\right|_{eq} \qquad \text{Eq.(4)}$$

where, $\dot{Q}_{skin}$ denotes the sum of convective, radiative, evaporative, and respiratory heat losses, i.e., $\dot{Q}_{skin} = \dot{Q}_{conv} + \dot{Q}_{rad} + \dot{Q}_{evap} + \dot{Q}_{res}$.

Substituting Eq.(3) into the whole-body energy balance [i.e., the Eq.(1)] yields

$$C\frac{dT_{cr}(t)}{dt} = -k\left[T_{cr}(t) - T_{cr,eq}(t)\right] \qquad \text{Eq.(5)}$$

This relation shown in Eq.(5) indicates that the rate of core temperature change is proportional to the instantaneous deviation from the environment-defined equilibrium value.

Dividing both sides of the Eq.(5) by C and defining the time constant $\tau = \frac{C}{k}$ gives

$$\frac{dT_{cr}(t)}{dt} = -\frac{1}{\tau}\left[T_{cr}(t) - T_{cr,eq}(t)\right] \qquad \text{Eq.(6)}$$

The thermal time constant τ characterizes the rate at which T_{cr} approaches equilibrium following an environmental step change. Eq.(6) describes a linear first-order low-pass response with time constant τ that encompasses both passive body heat storage and active thermoregulatory feedback. The time constant τ represents the characteristic response time for T_{cr} to approach a new equilibrium following an environmental step change in relative humidity (RH).

During each discrete humidity step of duration Δt, the equilibrium temperature $T_{cr,eq}$ is assumed to remain constant. The analytic solution of Eq.(6) for a step initiated at time $t = t_n$ is given by

$$T_{cr}(t) = T_{cr,eq,n} + \left[\left(T_{cr}(t_n) - T_{cr,eq,n}\right) \times e^{-\frac{(t-t_n)}{\tau}}\right] \qquad \text{Eq.(7)}$$

At the end of each step ($t_{n+1} = t_n + \Delta t$):

$$T_{cr,n+1} = T_{cr,eq,n} + (T_{cr,n} - T_{cr,eq,n}) \times e^{-\frac{\Delta t}{\tau}} \qquad \text{Eq.(8)}$$

Eq.(8) quantifies how far the body approaches equilibrium within each step. If Δt is sufficiently small, Eq.(8) can be approximated using the Euler form (23)

$$T_{cr,n+1} \approx T_{cr,n} + \frac{\Delta t}{\tau} \times (T_{cr,eq,n} - T_{cr,n}) \qquad \text{Eq.(9)}$$

When the environmental humidity change is rapid (i.e., $\frac{\Delta t}{\tau} \ll 1$), the system (i.e., human body) does not equilibrate between steps, and residual thermal disequilibrium accumulates, expressed as

$$\left.\frac{dT_{cr}}{dt}\right|_{n+1} > \left.\frac{dT_{cr}}{dt}\right|_{n} \qquad \text{if} \quad \frac{\Delta t}{\tau} \ll 1 \qquad \text{Eq.(10)}$$

where, $\left.\frac{dT_{cr}}{dt}\right|_{n+1}$ and $\left.\frac{dT_{cr}}{dt}\right|_{n}$ denote slopes of the core temperature change at the (n+1)th and nth step of a humidity ramp. It can therefore be deduced from Eq.(10) that the progressive acceleration in T_{cr} rise results in an apparent inflection, which reflects dynamic lag rather than true uncompensable heat stress. Detailed mathematical justification can be found in Supporting Information.

2.2 | Physiological verification study

2.2.1 | Sample size and power calculation

The primary comparison focused on differences in the critical inflection point of core temperature (T_{cr}) between two ramp protocols (aggressive-ramp and slow-ramp) and between sexes. Power analysis was performed based on expected sex differences, assuming a large expected effect size (Cohen's d = 0.8) and a paired-samples t-test. This analysis indicated that a minimum of 12 males and 12 females were required to achieve 80% statistical power at a two-tailed significance level of 0.05.

2.2.2 | Participants and ethical approval

Fourteen healthy young males (age: 23.6±2.0 yrs, height: 1.77±0.07 m, weight: 74.9±9.2 kg, body surface area: 1.92±0.15 m^2, body mass index: 23.9±1.5 kg/m^2) and 12 healthy young females (age: 22.5±2.1 yrs, height: 1.62±0.07 m, weight: 55.3±6.1 kg, body surface area: 1.58±0.10 m^2, body mass index: 21.1±2.4 kg/m^2), all nonsmokers and free from cardiovascular, metabolic, or thermoregulatory disorders, volunteered for this study. Female participants were tested during the follicular phase of their menstrual cycle (days 1–12 following the onset of menses), when endogenous progesterone levels are low. All female participants did not use hormonal contraceptives. Written informed consent was obtained from all participants prior to testing. The study was approved by the Institutional Review Board (IRB) of Xi'an University of Science and Technology (Approval No. XUST-IRB225034 and XUST-IRB225071) and conducted in accordance with the principles of the Declaration of Helsinki.

2.2.3 | Experimental design and rationale

Upon arrival, participants provided a urine sample to assess hydration status. Testing commenced only if urine specific gravity (USG) was ≤1.020, indicating euhydration (24). Participants with USG values above this threshold consumed an isotonic electrolyte solution and were re-tested until euhydration was achieved. Prior to chamber entry, participants confirmed a thermoneutral perception across all body regions, and their initial rectal temperature (T_{cr}) was required to be ≤ 37.1 °C. These procedures ensured that all trials began under comparable baseline hydration and thermal states. To maintain strict

control over the chamber's ambient conditions for the duration of each trial, a restroom facility was installed within the heat chamber. Participants were instructed that they had free access to this restroom at any time, thereby eliminating the experimental confound of temperature or humidity fluctuations associated with chamber exit and re-entry. The actual T_w in the chamber is calculated using the Stull equation (25).

Each participant completed two physiological trials (aggressive-ramp and slow-ramp) in a randomized, counterbalanced order, separated by at least one week. All experiments were conducted in a convective-type heat chamber, maintained at T_{db}=42 °C, with no appreciable radiant heat sources (e.g., infrared heaters or radiant panels) present inside the chamber. Participants remained seated throughout and performed light office tasks (e.g., reading, typing, watching movies, or using their phones). In the aggressive-ramp protocol, ambient relative humidity (RH) was initially set at 28% for 30 minutes, followed by a 2% RH increase every 5 minutes until the termination criterion was reached. In the slow-ramp protocol, participants first underwent a 4-hour equilibration phase at 40% RH, after which RH increased by 6% per hour from the 4th to 6th hour, and by 3% per hour thereafter until termination criteria were met.

The slow-ramp protocol was initiated at 40% RH to ensure experimental feasibility while minimizing non-thermal confounders. Initiating the ramp at lower RH levels (e.g., 28%, as used in the aggressive-ramp protocol) would have required exposures exceeding 12 hours to reach uncompensable heat stress (i.e., wet-bulb temperatures exceeding the compensable limit), even without progressing to the final humidity levels (88%) attained in the aggressive-ramp protocol. Such prolonged exposures would introduce additional physiological and behavioral influences (e.g., fatigue, circadian drift, prolonged fasting) that could obscure thermophysiological responses. Importantly, even if the same initial humidity (e.g., 28% RH) were imposed in both protocols, the exposure history would remain fundamentally different. In the aggressive-ramp protocol, participants resided at each humidity level for 5 minutes, whereas in the slow-ramp protocol the same RH was maintained for 60 minutes. Consequently, identical RH values correspond to markedly different thermal loads and physiological states, and subsequent environmental conditions diverge despite nominal matching of starting humidity.

Notably, although these ramp protocols are commonly described as ‘per-hour’ or ‘per-5-minute’ RH increases, each humidity adjustment was implemented as a discrete step. In practice, the chamber reached each new target RH within approximately 2–3 minutes. As a result, participants were exposed to a series of stepwise humidity transitions rather than a continuous environmental ramp. Each 3–10% RH increment constituted a transition between distinct environmental conditions, characterized by an

abrupt increase in ambient water vapor pressure. Under these conditions, the primary temporal determinant of thermophysiological responses is the dwell duration (Δt) at each humidity level, rather than the nominal ramp rate expressed on an hourly basis. Describing these protocols in terms of hourly RH increases is therefore potentially misleading, as physiological responses are governed by successive step changes rather than by a truly gradual ramp. Conceptually, this exposure structure is analogous to participants moving sequentially between a series of chambers, each maintained at a fixed humidity, rather than remaining within a single chamber experiencing a continuous humidity ramp. **Figure 1** presents a schematic overview of the two humidity-ramp protocols and the corresponding wet-bulb temperatures observed during each protocol.

----------*insert Figure 1 about here*----------

2.2.4 | Measurements

Hydration status was determined using a digital hand-held refractometer (PAL-1, Atago Co. Ltd., Tokyo, Japan; accuracy: ±0.2%). Rectal temperature (T_{cr}) was measured using a thermistor probe (YSI-401, YSI Inc., Yellow Springs, OH) inserted 10 cm beyond the anal sphincter. Mean skin temperature (T_{sk}) was obtained using iButtons (DS1992L, Maxim Integrated, Sunnyvale, CA; calibrated to accuracy: ±0.2 °C) affixed at the chest, upper arm, thigh, and calf, weighted according to Ramanathan's four-site equation (26). Heart rate (HR) was continuously recorded using chest-strap telemetry (Polar Vantage XL, Polar Electro Oy, Finland). Metabolic rate was assessed using a breath-by-breath metabolic system (Calibre Biometrics, Wellesley, MA) for 10 minutes after a 15-minute thermal stabilization period during which participants performed light office tasks in the heat chamber (27). Perceptual ratings of thermal sensation, thermal discomfort, skin wetness, and thirst sensation were obtained every 5–10 min using validated scales (**Figure S1**) (28). Environmental conditions (T_{db} and RH) were monitored continuously using three calibrated temperature–humidity data loggers (TH42W-EX, HHW Technology Co. Ltd., Shenzhen, China; temperature accuracy: ±0.1 °C; humidity accuracy: ±1.5%). The loggers were positioned at heights of 0.1 m, 0.6 m, and 1.1 m above the floor. Core temperature, skin temperature and heart rate were logged at 1-minute intervals throughout all trial phases.

2.2.5 | Termination criteria

Trials were immediately terminated if any of the following occurred: 1) T_{cr} reached or exceeded 38.6 °C; 2) onset of heat-related symptoms, including but not limited to involuntary hyperventilation, sustained piloerection, heat-related tetany, numbness, dizziness, nausea, confusion, or presyncope, as

identified through participant self-report or clinical observation by a certified nurse; 3) voluntary withdrawal by the participant; or 4) the total exposure duration reached 9 hours for slow-ramp and adaptive-ramp conditions, or 3 hours for aggressive-ramp conditions, reflecting the intensity and rate of humidity increase in each protocol. Upon termination, environmental heating was immediately halted, and participants were promptly removed to a cool indoor room (21–24 °C) for active recovery, including hydration and monitoring of vital signs to ensure safety.

2.2.6 | Data analysis

Individual T_{cr} data were smoothed using the *smooth* function with a smoothing parameter (*spar*) of 0.9 (17). The time derivative of T_{cr} (°C/h) was then computed to identify inflection points corresponding to the onset of uncompensable heat stress. The critical humidity limit was defined in ramp protocols as the environmental conditions at which an inflection in T_{cr} is observed. Comparisons between the two humidity-ramp protocols were performed to determine whether shorter dwell intervals (aggressive ramp, 2% per 5 min) produced systematically lower apparent critical wet-bulb temperature ($T_{\mathrm{w,critical}}$) compared to the slow-ramp protocol (6% per hour). Because each participant completed both protocol trials, differences $T_{\mathrm{w,critical}}$ between the aggressive-ramp and slow-ramp protocols were analyzed separately for females (n=12) and males (n=14) using paired-samples t-tests. Effect sizes were expressed as Cohen's d (calculated as the mean difference divided by the standard deviation of the differences). Sex differences in $T_{\mathrm{w,critical}}$ and body surface area-to-mass ratio were examined separately for each ramp protocol using independent-samples t-tests (Welch's correction for unequal variances). All tests were two-tailed with α=0.05 and all statistical analyses were conducted in IBM SPSS Statistics (version 29.0.1.0), with significance set at P<0.05. Data are presented as means ± SD (standard deviation) unless otherwise specified.

2.2.7 | Inflection point determination

Earlier studies (8–16) identified the compensable–uncompensable transition visually based on curvature in the core temperature trace. Although pioneering, this graphical approach relied on subjective judgment and exhibited limited reproducibility, particularly when T_{cr} increased gradually or was affected by transient fluctuations. In the present study, the inflection point was defined objectively as the first time the smoothed T_{cr} slope reached or exceeded 0.25 °C/h and remained above this threshold thereafter. This criterion minimizes subjectivity, improves reproducibility, and aligns the detected inflection with the physiological onset of sustained uncompensable heat strain. To assess robustness, sensitivity analyses were performed using alternative slope thresholds (0.15, 0.20, 0.25,

and 0.30 °C/h; see **Table S1** in Supporting Information). Results confirmed that 0.25 °C/h provided stable and physiologically consistent estimates, whereas looser or stricter thresholds either advanced the transition unrealistically or delayed it toward higher core temperatures, potentially obscuring the early onset of uncompensable heat stress.

2.2.8 | Validation of CELs derived from slow- and adaptive-ramp protocols

To validate the CELs derived from the slow-ramp and adaptive-ramp protocols (see Section **3.2**), additional prolonged stable-exposure trials were conducted at T_{db}=42 °C using independent cohorts of healthy young participants. Fourteen males (age: 24.4±1.8 yr; height: 1.76±0.04 m; body mass: 70.3±4.9 kg; BMI: 22.8±1.5 kg/m^2) and fourteen females (age: 23.0 ± 1.8 yr; height: 1.59 ± 0.06 m; body mass: 51.3 ± 5.7 kg; BMI: 20.4 ± 2.2 kg/m^2) were recruited under the same inclusion criteria and ethical approvals as those applied in the main study.

For males, exposures targeted T_w=32.7 °C (expected compensable) and T_w=34.3 °C (expected uncompensable); for females, target T_w values were 33.1 °C (expected compensable) and 34.6 °C (expected uncompensable). Participants remained seated in light clothing with *ad libitum* electrolyte intake, and trials lasted up to 8 hours or until predefined safety endpoints were reached (T_{cr} ≥ 38.6 °C, heart rate ≥ 90% age-predicted maximum, severe discomfort or heat-related tetany, or participant voluntary withdrawal). Rectal temperature (T_{cr}), skin temperature, heart rate, and perceptual scales were monitored continuously.

Compensability was defined as T_{cr} stabilization (< 0.10 °C/h slope after 3 hours and maintained for at least 20 min), whereas uncompensability was defined as a sustained rise in T_{cr} (> 0.10 °C/h) without evidence of plateau. These slope-based criteria were previously assessed using sensitivity analyses in prolonged exposure studies (17, 28), which demonstrated that compensability classification was robust to reasonable variations in the slope threshold and aligned with physiologically plausible patterns of core temperature stabilization or sustained increase.

3 | Results

3.1 | Physiological interpretation of the model

The model conceptualizes the human thermoregulatory system as a first-order dynamic process governed by a single thermal time constant (τ), which defines the rate at which the body approaches thermal equilibrium. Two contrasting response regimes emerge depending on the relationship between

the dwell interval (Δt) and this physiological time constant. When the dwell interval is short relative to the body's thermal inertia ($\Delta t \ll \tau$), core temperature does not fully equilibrate at each new humidity level before the next increment occurs. As a result, residual deviations between the instantaneous equilibrium temperature and the actual T_{cr} accumulate across successive steps. This cumulative lag manifests as an apparent acceleration in the rise of T_{cr}, producing an early inflection point that may be erroneously interpreted as a physiological limit of heat tolerance. Conversely, when the dwell interval is sufficiently long relative to the time constant ($\Delta t \gtrsim \tau$), T_{cr} has adequate time to approach equilibrium within each step, thereby minimizing transient deviations. Under these conditions, the temporal evolution of core temperature more accurately follows the equilibrium trajectory, yielding a smoother and more physiologically representative response to incremental humid heat stress.

3.2 | Empirical derivation of CELs from aggressive- and slow-ramp protocols

Critical environmental limits (CELs), expressed as critical wet-bulb temperature ($T_{w,critical}$), differed substantially depending on the duration of humidity increments (Δt). Core temperature increased most rapidly and reached critical levels earlier during the aggressive-ramp protocol than during the slow-ramp protocol.

----------*insert Figure 2 about here*----------

Across the 14 male participants, the mean critical wet-bulb temperature ($T_{w,critical}$) in the aggressive-ramp condition (Δt =5 min) was 29.9±1.6 °C, whereas the slow-ramp condition (Δt =60 min) yielded a significantly higher $T_{w,critical}$ value of 33.4±0.5 °C (mean difference: 3.4±1.9 °C; P<0.001, Cohen's d=1.78; see **Figures 2A–2B** and **Figures S2–S3**). Similarly, in female participants (n=12), $T_{w,critical}$ was significantly lower in the aggressive-ramp (30.3±0.9 °C) than in the slow-ramp condition (33.8±0.5 °C, mean difference: 3.5±0.9 °C; P<0.001; Cohen's d=3.84; **Figures 2C–2D** and **Figures S2–S3**). These differences highlight the influence of thermal inertia on the apparent timing of physiological inflection points. Consistent with dynamic thermal modelling, short ramp durations create cumulative thermal lag, resulting in an earlier inflection in rectal temperature and thus lower apparent $T_{w,critical}$ values. In contrast, prolonged humidity increments allow the body to approach thermal equilibrium at each step, shifting the apparent critical threshold to higher T_w values.

Under the aggressive-ramp protocol, no significant difference in $T_{w,critical}$ was observed between females (30.3±0.9 °C) and males (29.9±1.6 °C; Welch's $t(20.2) = 0.69$, two-tailed P=0.497, one-tailed P=0.248, Cohen's d=0.26). In contrast, under the slow-ramp protocol, females exhibited higher $T_{w,critical}$ values than males (33.8±0.5 °C vs. 33.4±0.5 °C; Cohen's d=0.80). The difference approached

statistical significance in a two-tailed test (Welch's $t(23.6) = 2.03$, $P=0.053$) and reached significance in a one-tailed test ($P=0.027$), consistent with our a-priori directional hypothesis that females would show higher values. This difference was accompanied by a large effect size (Cohen's $d=0.80$), suggesting a potentially meaningful sex difference under slower humidity ramp conditions.

----------*insert Figure 3 about here*----------

Further, the time required for T_{cr} to stabilize under constant ambient temperature conditions was empirically determined using three relative humidity (RH) increment levels (3%, 6% and 10%), following full initial equilibration of T_{cr}. The approach was termed the **adaptive ramp protocol**. **Figure 3** illustrates the temporal evolution of rectal temperature (T_{cr}) in six representative male participants and three female participants under the adaptive ramp protocol at T_{db}=42 °C. In **Figures 3A–3C**, three participants achieved a re-stabilized rectal temperature approximately 38–91 minutes after the first 3% RH increment following the initial stabilization period. Specifically, the participant in **Figure 3B** re-established T_{cr} equilibrium at 356 and 436 min following the second and third 3% RH increments, respectively. In contrast, the participant in **Figure 3C** achieved T_{cr} re-stabilization at 194, 246, 316, 357 and 388 min following five successive 3% RH increments applied after the initial equilibration phase (0–181 min). Consistently, in **Figures 3D–3F**, T_{cr} required approximately 98–197 min to re-establish steady-state conditions following the first 10% RH increment. Notably, the participant shown in **Figure 3E** re-stabilized after 206 minutes (i.e., 502 min) following the second RH increment (6%) initiated at 296 min, after an initial 10% RH step. For female participants, **Figures 3G–3I** illustrate the stabilization of T_{cr} at successive time points following humidity increments. In **Figure 3G**, a representative female participant re-established T_{cr} stabilization at 222, 270, 308, 339, and 371 minutes after the initial equilibration, corresponding to five successive 3% RH increments. Similarly, in **Figure 3H**, another participant achieved stabilization at 217, 301, and 361 minutes following three 3% RH increments. In **Figure 3I**, a third female participant reached stabilization at 219 minutes (first ramp increment), 272 minutes (second ramp increment), and remained stabilized following the subsequent five 3% RH increments from 303 minutes to 425 minutes. These observations demonstrate that although the heat chamber achieved 3–10% RH increments within 3–5 min, physiological equilibration of T_{cr} occurred much more slowly than previously assumed. Collectively, these results indicate that conventional humidity-ramp protocols with 5–10 min step durations are far insufficient to allow T_{cr} equilibration and may therefore underestimate the true critical environmental limits (CELs).

Inflection points identified under the adaptive ramp protocol ranged from 33.4–34.0 °C in male participants, whereas three representative females exhibited higher values of 33.8–34.5 °C (i.e., RH stepwise increments of 3-10% were applied only after prior T_{cr} stabilization) (**Figure 3**). These $T_{w,critical}$ values are very similar to those observed under the slow ramp protocol (males: 33.4±0.5 °C; females: 33.8±0.5 °C) and substantially higher than those from the aggressive-ramp protocol. Although T_{cr} progression under the slow-ramp protocol (with RH increments every hour) did not fully stabilize in many trials, the slow-ramp protocol still yielded $T_{w,critical}$ values comparable in precision to those obtained from the adaptive ramp protocol. Notably, some trials in **Figures 3A** and **3E** did not show an inflection point even after 9 hours of exposure. Nevertheless, the slow-ramp protocol demonstrated reliable performance in determining physiologically accurate $T_{w,critical}$ values, consistent with those observed in documented prolonged stable exposures (18, 19, 28).

3.3 | CEL validation against prolonged stable exposures

Prolonged stable-exposure trials at fixed T_{db}=42 °C confirmed the accuracy of CELs derived from the slow-ramp and adaptive-ramp protocols. In males (n=14), exposures at T_w=32.6±0.4 °C resulted in T_{cr} stabilization (< 0.10 °C/h slope after 5.8 hours), indicating compensable heat stress, whereas T_w=34.3±0.2 °C produced sustained T_{cr} rise (>0.10 °C/h without plateau), consistent with uncompensable conditions (**Figures 4A** and **4B**). Similarly, in females (n=14), T_w=32.9±0.4 °C was compensable with near-plateau T_{cr} dynamics (< 0.10 °C/h slope after 4.2 hours), while T_w=34.6±0.4 °C led to progressive uncompensable heat storage (**Figures 4C** and **4D**) . These findings align closely with the slow-ramp inflection points (males: 33.4 °C [32.8–34.2 °C]; females: 33.8 °C [33.0–34.3 °C]) and adaptive-ramp ranges (males: 33.4–34.0 °C; females: 33.8–34.5 °C), demonstrating that slower/adaptive ramp structures yield physiologically valid CEL thresholds. In contrast, the aggressive-ramp protocol's lower CELs (males: ~29.9 °C; females: ~30.3 °C) would misclassify the tested T_w=32.7 °C (males) and T_w=33.1 °C (females) conditions—along with intermediate ranges (e.g., ~30.0–32.7 °C in males and ~30.4–33.0 °C in females)—as uncompensable, despite clear evidence of compensability under prolonged stable exposure.

----------*insert Figure 4 about here*----------

3.4 | Sensitivity analysis

The first-order dynamical model highlights that the ratio $\Delta t/\tau$ (i.e., the ratio of step dwell time to the physiological time constant) determines whether T_{cr} can approach equilibrium at each stage. When

$\Delta t/\tau \ll 1$, equilibration fails and residual deviations accumulate, yielding an apparent acceleration and a premature inflection in T_{cr}. This phenomenon constitutes a dynamic lag artifact rather than true physiological collapse.

Empirically derived estimates of the core temperature time constant (τ), obtained after an initial full equilibration of T_{cr} in the humidity ramp approach, ranged from approximately 1.0 hour to over 3.3 hours, depending on metabolic rate, hydration status, and thermoregulatory efficiency. Consequently, step durations of 5–10 minutes, commonly used in ramp-based studies, likely place participants in the aggressive-ramp regime, where such artefacts are inevitable (8, 9, 11, 13, 16). We therefore recommend either empirical estimating τ for each cohort or performing sensitivity analyses to verify the robustness of threshold estimates across plausible τ values. **Table 1** presents the sensitivity of the dynamic response to step duration relative to the physiological time constant.

----------insert Table 1 about here----------

4 | Discussion

This study demonstrates that the apparent CEL (i.e., $T_{w,critical}$ values) observed in humidity ramp protocols is strongly influenced by the temporal structure of the environmental change. Our first-order dynamic model reveals that when the rate of relative humidity (RH) increase exceeds the body's intrinsic thermal response time (17–19, 28, 29), the rise in core temperature (T_{cr}) accelerates across successive steps. Under such conditions, frequent small humidity increments force the body to continually "chase" a moving target equilibrium, producing apparent inflection points that reflect dynamic lag artifacts rather than true thermoregulatory failure. Conversely, when each step is maintained long enough to permit partial or full equilibration, these transient discrepancies diminish, and the T_{cr} trajectory becomes smoother and physiologically interpretable.

The ratio of step duration (Δt) to the thermal time constant (τ) offers a dimensionless index of ramp adequacy. When $\Delta t/\tau \ll 0.2$, dynamic lag dominates, yielding premature inflections and artificially low apparent thresholds; ratios between $0.2 \leq \Delta t/\tau < 0.5$ allow partial equilibration, while $\Delta t/\tau \gtrsim 0.5$ approximates quasi-steady-state conditions with minimal artifacts. Empirically, a ratio near 0.3 achieved partially stable core temperature responses without excessively prolonging the protocol. Estimating τ during the initial equilibration phase can therefore guide individualized ramp pacing, while post hoc dynamic correction models may further approximate equilibrium T_{cr} values without requiring longer exposures.

A critical methodological insight is that humidity protocols, despite being nominally described as progressive 'ramps' (e.g., 6%/10% per hour or 2% every 5 min), are implemented in practice as rapid stepwise transitions, with chamber setpoints achieved in approximately 2–3 minutes. Participants thus experience discrete environmental steps, each imposing an instantaneous shift in equilibrium core temperature ($T_{cr,eq}$). Under these conditions, the physiologically decisive parameter is the dwell duration (Δt) at each step. When Δt is short relative to the body's thermal time constant (τ), incomplete equilibration is unavoidable. This mismatch ($\Delta t/\tau \ll 1$) causes T_{cr} to continually chase a shifting equilibrium, producing cumulative thermal lag, characteristic acceleration in T_{cr} rise, and premature inflection points that traditional ramp protocols misinterpret as the onset of uncompensable heat stress.

Although the model simplifies the human thermoregulatory system to a first-order process characterized by a single time constant and linear heat exchange, it effectively captures the essential delay dynamics linking environmental perturbations to physiological responses. Human thermoregulation involves inherently nonlinear processes such as sweating kinetics, core–skin coupling, and delayed feedback in vasomotor and sudomotor control (30–33). Nonetheless, the present first-order framework isolates the temporal dimension of these higher-order complexities. As such, it provides a tractable and physiologically interpretable foundation for refining humidity-ramp protocols and improving the validity of human heat tolerance assessments.

The classic formulation by Belding and Kamon (8) emphasized the necessity of initial equilibration, noting that core temperature could require "*more than 2 hours to re-stabilize*" at critical vapor pressure levels. To reduce the labor-intensive nature of the full steady-state method, they introduced a shortcut approach—increasing humidity by approximately 1 mm Hg (≈2% RH at 42 °C) every 10 minutes following an initial hour of equilibration. While this adjustment acknowledged the importance of stabilization upon chamber entry, it did not extend the principle to subsequent humidity increments. As a result, the ongoing influence of physiological equilibration on determining critical environmental limits (CELs) was not fully appreciated. Our empirical data demonstrate that this assumption is invalid: even small humidity increases (e.g., 3%) required approximately 0.63–1.52 h for T_{cr} to re-stabilize (**Figure 3**). Hence, shortcut ramp protocols progress much faster than the body's thermal time constant, leading to premature inflection points that misrepresent the true onset of uncompensable heat stress. Consistent with this interpretation, studies employing short dwell times (10, 11, 13–16) have reported $T_{w,critical}$ values of 26.0–32.3 °C in unacclimatized young adults—substantially lower than steady-state-derived thresholds of $T_{w,critical}$ =33–34 °C (28, 34, 35). Because prior ramp studies also implemented humidity transitions as rapid step changes with short dwell intervals, their reported 'inflection points' likely reflect the same dynamic lag artifacts identified here.

Figure 3G illustrates a representative time course of T_{cr} in a female participant during a stepwise humidity ramp protocol with adaptive dwell times. Each humidity increment was 3% RH, with the duration of each step extended until T_{cr} reached a steady state, operationally defined as $|dT_{cr}/dt| \leq 0.1$ °C over 30-minute window. The inflection point—indicating the onset of sustained upward drift in T_{cr} and thus the critical wet-bulb temperature ($T_{w,critical}$)—was determined using the criterion $|dT_{cr}/dt| > 0.25$ °C/h. In this case, the inflection occurred at 465 min (total trial duration: 480 min), corresponding to $T_{w,critical}$= 33.8 °C. This individual $T_{w,critical}$ value matches precisely the group mean for young adult females under the slow-ramp protocol described in this study (33.8±0.5 °C), supporting the conclusion that slow-ramp protocols with sufficiently prolonged dwell times yield accurate, physiologically representative estimates of human heat tolerance limits by minimizing the confounding effects of cumulative thermal disequilibrium. A schematic overview of an ideal adaptive humidity-ramp protocol—one that maintains each step until T_{cr} reaches steady state to isolate transient thermal dynamics—is provided in **Figure S6**. In the example shown in **Figure 3G**, the estimated time constant of the core temperature response ($\tau \approx 70$ min) yields a $\tau/\Delta t$ ratio ranging approximately 0.43 (for the shortest step, Δt=30 min) to 2.61 (for the longest step, Δt=183 min) across the six humidity increments. The fact that $\tau/\Delta t$ values exceeded 0.30 after the initial full T_{cr} stabilization in later steps further validates the proposed $\tau/\Delta t$ ratio as a robust index of ramp adequacy: values substantially greater than ~0.3 indicate sufficient equilibration at each humidity step, reducing cumulative disequilibrium and yielding more ecologically valid CEL estimates.

Comparison between the aggressive (Δt = 5 min) and slow (Δt = 60 min) ramp regimens underscores the importance of temporal pacing for accurately estimating CELs. Using the slow-ramp protocol, $T_{w,critical}$ values were identified as 33.4 °C in males and 33.8 °C in females. These values were subsequently validated using prolonged stable exposures at T_{db}=42 °C, where T_w=32.7 °C (males) and 33.1 °C (females) resulted in T_{cr} stabilization (i.e., compensable conditions), whereas T_w=34.3 °C (males) and 34.6 °C (females) produced sustained increases in T_{cr} (i.e., uncompensable conditions). These thresholds align closely with previously reported compensable–uncompensable boundaries derived from prolonged stable exposures in unacclimatized young males ($T_{w,critical}$=33.8–34.0 °C; all T_w values were recalculated using the Stull method (25) at comparable low-to-moderate metabolic rates of 1.2– 2.0 METs (19, 28, 34, 35). In contrast, the aggressive-ramp systematically underestimated these thresholds due to thermal inertia and cumulative physiological disequilibrium. At T_{db}=42 °C, each 3% RH increase corresponds to an approximate 0.7 °C rise in T_w, which is sufficient to overshoot the narrow 33–34 °C transition zone in a single step. This illustrates the inherent difficulty of precisely

determining true heat tolerance limits in the absence of prolonged dwell times or stable exposures that permit complete physiological equilibration.

Under the aggressive-ramp protocol (total duration ≤ 3 h), no significant sex difference in $T_{w,critical}$ was observed, likely due to rapid humidity increments that induced substantial thermal lag and transient heat storage. In this protocol, absolute body mass (acting as a heat sink) and higher metabolic heat production in males dominated responses, overshadowing morphological advantages. In contrast, the slow-ramp protocol (8–9 h duration) allowed for closer thermal equilibrium at each step, enabling females' higher surface area-to-mass ratio (0.0287±0.0018 m²/kg [females] vs. 0.0257±0.0012 m²/kg [males], two-sided P<0.001; Cohen's d=2.023) and lower absolute body mass to facilitate greater relative dry and evaporative heat loss in humid conditions (55.3±6.1 kg [females] vs. 74.9±9.2 kg [males]). This reduced metabolic heat production during seated/light activity, manifesting as modestly higher $T_{w,critical}$ in females (~0.4–0.5 °C advantage). These findings align with biophysical principles suggesting that such advantages are more evident during prolonged humid exposures when steady-state heat balance can be approximated (12, 13, 36).

These protocol-specific patterns underscore that apparent sex differences in heat tolerance are time-dependent and more pronounced when ramp durations minimize thermal inertia. Females typically display lower absolute sweat rates but more efficient evaporative cooling per unit surface area (i.e., reduced 'wasted' sweat) in limiting humid conditions. Such biophysical factors have long been proposed to confer advantages to females in warm-humid exposures when fitness and acclimatization are comparable (7, 36). These findings align with reports from the PSU HEAT project, which documented modest or context-dependent sex influences on $T_{w,critical}$ among young healthy adults during minimal-to-light activity (~0.8 MET) in hot environments, with morphology (e.g., body size/surface area) often contributing to observed variance (12–14). The modest female advantage observed here may reflect the specific seated/light-office paradigm, slower humidity ramp (allowing closer thermal equilibrium), and fixed dry-bulb temperature (42°C) employed. Further investigation in diverse cohorts, activity levels, and environmental conditions is needed to clarify the relative roles of morphology, physiology, and protocol design.

4.1 | Physiological and methodological implications

We propose the ratio $\Delta t/\tau$ as a dimensionless index of protocol adequacy, where Δt represents the dwell duration of each humidity step and τ is the physiological time constant for core temperature equilibration. When $\Delta t/\tau < 0.2$, ramp protocols induce significant dynamic artifacts due to incomplete equilibration. Values of $0.2 \leq \Delta t/\tau < 0.5$ allow partial equilibrium responses, whereas $\Delta t/\tau \geq 0.5$

approximates quasi–steady-state conditions with minimal artifacts. Empirically, a ratio of approximately 0.3 was sufficient to achieve partially stable core temperature responses without excessively prolonging exposure. Estimating τ from the exponential rise of T_{cr} during the initial equilibration phase allows individualized ramp pacing aligned with each participant's thermophysiological response capacity.

This framework explains why rapid humidity-ramp protocols consistently yield artificially low CELs and underscores the need for standardized ramp parameters across laboratories. Inflection-based thresholds should be interpreted as transient artifacts rather than steady-state physiological limits. In this context, prolonged stable exposures remain the definitive benchmark for defining true compensability and calibrating predictive models, occupational exposure limits (OELs), and wearable heat-strain algorithms (37).

The methodological implications are significant. Conventional aggressive (or rapid) humidity-ramp studies implicitly assume adequate equilibration between increments, yet our data demonstrate that typical 5–10-minute dwell times are far shorter than the body's equilibration period (38). At $T_w \approx$ 31.7 °C (T_{db} = 42 °C), T_{cr} required approximately ≥ 1.63 hours (98 min) to re-establish steady-state conditions after a 10% RH increase during the first stepwise increment (**Figures 3D–3F**). Consequently, the apparent "inflection point" observed in ramp experiments largely reflects cumulative transient heat storage rather than the true transition to uncompensable heat stress. This dynamic lag produces artificially steep T_{cr} trajectories and systematically underestimates human heat tolerance.

Accordingly, aggressive humidity-ramp protocols should be viewed as rapid yet approximate methods for determining environmental compensability thresholds. To derive true, physiologically valid estimates, each step must be maintained until at least partial steady-state equilibration is achieved, as seen in the slow-ramp protocol. While the adaptive ramp protocol is ideal for accurately quantifying human heat tolerance, some heat-tolerant participants may require over 10 hours to identify an inflection point. Ideally, the adaptive ramp protocol should be prioritized for its precision. However, considering the time burden and physiological strain on participants, the slow-ramp protocol serves as the best alternative, offering a balance between accuracy and feasibility. Although time-consuming, both approaches provide reliable representations of environmental compensability, with the adaptive ramp protocol delivering the most accurate and precise estimates. Both protocols, however, still rely on prolonged stable exposure to verify their accuracy, minimizing transient effects and capturing true physiological limits. Thus, prolonged stable exposure remains the methodological gold standard for

quantifying human heat tolerance but offers an ecologically valid approach for assessing heat stress under realistic environmental conditions (17, 39, 40).

4.2 | Limitations and future directions

This study identified a key methodological artifact in the classic humidity-ramp protocol, using a homogeneous cohort of young adults at a representative dry-bulb temperature. This design intentionally minimized inter-individual variability to isolate ramp-timing effects, but it limits generalizability of the reported absolute *critical environmental limit* (CEL) values, given known variation in thermoregulatory function with age, acclimatization, and other factors (40, 41).

Importantly, the artifact—premature apparent T_{cr} inflection point due to insufficient dwell time—is a protocol flaw, not a population-specific trait. Human thermal equilibration follows a universal time constant (τ) (17); core temperature cannot instantaneously track rapid environmental changes in any individual, regardless of age, sex, or fitness. Thus, inadequate dwell time ($\Delta t/\tau \ll 1$) systematically biases the classic ramp protocol toward underestimating true CEL across all populations. Although exact CEL values at a given T_{db} may vary between groups, short-dwell ramp protocols will consistently underestimate group-specific limits due to this timing artifact. The $\Delta t/\tau$ framework presented here offers a practical correction for future studies, especially in older adults and other vulnerable cohorts, enabling more accurate and comparable estimates of environmental tolerance.

5 | Conclusion

Humidity-ramp protocols have long served as practical tools for assessing safe occupational exposure limits under hot environments and have recently been applied to estimate critical environmental limits (CELs) of human heat tolerance. However, their validity is inherently limited by thermal disequilibrium: when environmental change outpaces physiological equilibration, apparent inflection points largely reflect dynamic lag rather than true uncompensability, typically underestimating heat tolerance. CELs obtained from short-duration (aggressive) ramps should therefore be interpreted cautiously. Accurate determination of physiological heat tolerance requires either prolonged stable exposures—the gold standard—or the slow-ramp protocol presented here, which better approximates thermal equilibrium. Aggressive humidity-ramp protocols should not be relied upon as standalone methods for defining precise heat tolerance limits. Prolonged stable exposure remains the primary benchmark for establishing ecologically valid thresholds of human environmental compensability and should guide future research in this domain.

Author contributions

F.F.W. conceived the study, developed the model, designed experiments, prepared figures and illustrations, acquired funding, and drafted the manuscript and Supporting Information. Y.X. performed experiments, analyzed data, prepared figures, and revised the manuscript. H.W., M.C., X.H., B.W., and X.S. performed experiments, analyzed data, and revised the manuscript. All authors reviewed and approved the final version of the manuscript.

Acknowledgments

This research study was supported by the National Excellent Young Scientist Program (Grant No. 6119924022, to F.F.W.). We sincerely thank all participants of the study for their time and invaluable contributions.

Conflict of interest statement

The authors declare no conflicts of interest, financial or otherwise.

Data availability statement

Data are available upon request from the corresponding author (F.F.W.).

Supporting information

Additional supporting information is submitted as part of the peer review process.

Author ORCID

Fèlix Faming Wang: 0000-0002-2945-4685

Yi Xu: 0009-0003-9555-8778

Haojian Wang: 0009-0004-1469-7539

References

1. **Rahmstorf S, Coumou D.** Increase of extreme events in a warming world. *Proc Natl Acad Sci U S A* 108: 17905–17909, 2011. doi:10.1073/pnas.1101766108.
2. **Pandolf KB.** Aging and human heat tolerance. *Exp Aging Res* 23: 69–105, 1997. doi:10.1080/03610739708254027.
3. **Taylor NAS.** Human heat adaptation. *Compr Physiol* 4: 325–365, 2014. doi:10.1002/j.2040-4603.2014.tb00547.x.
4. **Bouchama A.** Redefining human heat limits: integrating molecular and evolutionary physiology. *J Physiol*. doi:10.1113/JP289455.
5. **Wang F.** Redefining human heat limits requires accurate quantification of core temperature threshold. *J Physiol*. doi:10.1113/JP290359.
6. **Sherwood SC, Huber M.** An adaptability limit to climate change due to heat stress. *Proc Natl Acad Sci U S* A 107: 9552–9555, 2010. doi:10.1073/pnas.0913352107.
7. **Kenney WL, DeGroot DW, Holowatz LA.** Extremes of human heat tolerance: life at the precipice of thermoregulatory failure. *J Therm Biol* 29: 479–485, 2004. doi:10.1016/j.jtherbio.2004.08.017.
8. **Belding HS, Kamon E**. Evaporative coefficients for prediction of safe limits in prolonged exposures to work under hot conditions. *Fed Proc* 32: 1598–1601, 1973.
9. **Kamon E.** Empirical definition of limit to work in hot environments for women. *Proc Hum Factors Soc Annu Meet* 20: 290–293, 1976. doi:10.1177/154193127602001407.
10. **Cottle RM, Lichter ZS, Vecellio DJ, Wolf ST, Kenney WL.** Core temperature responses to compensable versus uncompensable heat stress in young adults (PSU HEAT Project). *J Appl Physiol* 133: 1011–1018, 2022. doi:10.1152/japplphysiol.00388.2022.
11. **Vecellio DJ, Wolf ST, Cottle RW, Kenney WL.** Evaluating the 35°C wet-bulb temperature adaptability threshold for young, healthy subjects (PSU HEAT Project). *J Appl Physiol* 132: 340–345, 2022. doi:10.1152/japplphysiol.00738.2021.
12. **Wolf ST, Folkerts MA, Cottle RM, Daanen HAM, Kenney WL.** Metabolism- and sex-dependent critical WBGT limits at rest and during exercise in the heat. *Am J Physiol Regul Integr Comp Physiol* 321: R295–R302, 2021. doi:10.1152/ajpregu.00101.2021.
13. **Wolf ST, Cottle RM, Vecellio DJ, Kenney WL.** Critical environmental limits for young, healthy adults (PSU HEAT Project). *J Appl Physiol* 132: 327–333, 2022. doi:10.1152/japplphysiol.00737.2021.
14. **Wolf ST, Havenith G, Kenney WL**. Relatively minor influence of individual characteristics on critical wet-bulb globe temperature (WBGT) limits during light activity in young adults (PSU HEAT Project). *J Appl Physiol* 134: 1216–1223, 2023. doi:10.1152/japplphysiol.00657.2022.
15. **Meade RD, Notley SR, Kenny GP.** Time to reach equilibrium deep body temperatures in young and older adults resting in the heat: a descriptive secondary analysis. *Am J Physiol Regul Integr Comp Physiol* 327: R369–R377, 2024a. doi:10.1152/ajpregu.00089.2024.

16. **Meade RD, O'Connor FK, Richards BJ, Tetzlaff EJ, Wagar KE, Harris-Mostert RC, Egube T, McCormick J, Kenny, GP.** Validity of a humidity ramp protocol for identifying environmental limits of human thermoregulatory compensability. *Med Sci Sports Exerc* 56: 19–20, 2024b. doi:10.1249/01.mss.0001052652.27698.3d.
17. **Wang F, Xu H, Lei TH, Xu Y, Wang H, Wang L.** Defining human thermoregulation limits: a critical evaluation of predictive models using healthy young adults. *Am J Physiol Regul Integr Comp Physiol* 329: R524–R533, 2025. doi:10.1152/ajpregu.00108.2025.
18. **Wyndham CH, Williams CG, Morrison JF, Heyns AJA, Siebert J.** Tolerance of very hot humid environments by highly acclimatized Bantu at rest. *Br J Ind Med* 25: 22–39, 1968. doi:10.1136/oem.25.1.22.
19. **Wyndham CH, Strydom NB, Heyns AJ, Rensburg AJ.** Tolerance times of high wet bulb temperatures by acclimatised and unacclimatised men. *Environ Res* 3: 339–352, 1970. doi:10.1016/0013-9351(70)90027-7.
20. **Gagge AP, Gonzalez RR.** Mechanisms of heat exchange: biophysics and physiology. *In: Terjung R, ed. Comprehensive Physiology* 2011: 45–84. doi:10.1002/j.2040-4603.1994.tb01150.x.
21. **Brebner DF, Kerslake DM, Waddell JL.** The effect of atmospheric humidity on skin temperature & sweat rates of resting men at two ambient temperatures. *J Physiol* 144: 299–306, 1958. doi: 10.1113/jphysiol.1958.sp006102.
22. **Clifford J, Kerslake DM, Waddell JL.** The effect of wind speed on maximum evaporative capacity in man. *J Physiol* 147: 253–259, 1959. doi: 10.1113/jphysiol.1959.sp006240.
23. **Stewart J.** Calculus: early transcendentals. 8th ed. *Kentucky, USA: Cengage Learning*; 2015.
24. **Oppliger RA, Magnes SA, Popowski LA, Gisolfi CV.** Accuracy of urine specific gravity and osmolality as indicators of hydration status. *Int J Sport Nutr Exerc Metab* 15: 236–251, 2005. doi:10.1123/ijsnem.15.3.236.
25. **Stull R.** Wet-bulb temperature from relative humidity and air temperature. *J Appl Meteorol Climatol* 50: 2267–2269, 2011. doi:10.1175/JAMC-D-11-0143.1.
26. **Ramanathan NL.** A new weighting system for mean surface temperature of the human body. *J Appl Physiol* 19: 531–533, 1964. doi:10.1152/jappl.1964.19.3.531.
27. **Van Hooren B, Souren T, Bongers BC.** Accuracy of respiratory gas variables, substrate, and energy use from 15 CPET systems during simulated and human exercise. *Scand J Med Sci Sports* 34: e14490, 2024. doi:10.1111/sms.14490.
28. **Wang F, Wang H, Xu Y, Han L, Shen X, Zhai Y, Zhang X, Liang Z, Hong B, Ma P, Zhao Z**. Mapping human survivability at extreme wet-bulb temperatures 32–35°C. *bioRxiv*. 2025: 2025.09.22.677706. doi:10.1101/2025.09.22.677706.
29. **Strydom NB, Wyndham CH, Williams CG, Morrison JF, Bredell GA, Benade AJ, Von Rahden M.** Acclimatization to humid heat and the role of physical conditioning. *J Appl Physiol* 21: 636–642, 1966. doi:10.1152/jappl.1966.21.2.636.

30. **Wyss CR, Brengelmann GL, Johnson JM, Rowell LB, Niederberger M.** Control of skin blood flow, sweating, and heart rate: role of skin vs. core temperature. *J Appl Physiol* 36: 726–733, 1974. doi:10.1152/jappl.1974.36.6.726.
31. **McCook RD, Wurster RD, Randall WC.** Sudomotor and vasomotor responses to changing environmental temperature. *J Appl Physiol* 20: 371–378, 1965. doi:10.1152/jappl.1965.20.3.371.
32. **Bini G, Hagbarth KE, Hynninen P, Wallin BG**. Thermoregulatory and rhythm-generating mechanisms governing the sudomotor and vasoconstrictor outflow in human cutaneous nerves. *J Physiol* 306: 537–552, 1980. doi:10.1113/jphysiol.1980.sp013413.
33. **Taylor NAS, Nykvist Å, Powers N, Caldwell JN.** Thermoeffector threshold plasticity: the impact of thermal pre-conditioning on sudomotor, cutaneous vasomotor and thermogenic thresholds. *J Therm Biol* 83: 37–46, 2019. doi:10.1016/j.jtherbio.2019.05.001.
34. **Wyndham CH, Strydom NB, Morrison JF, Du Toit FD, Kraan JG.** Responses of unacclimatized men under stress of heat and work. *J Appl Physiol* 6: 681–690, 1954. doi:10.1152/jappl.1954.6.11.681.
35. **Wang H, Xu Y, Xie T, Wang FF.** Standardizing core temperature reporting for indoor overheating research: effects on thermal equilibrium duration and compensability. *Manuscript submitted*.
36. **Shapiro Y, Pandolf KB, Avellini BA, Pimental NA, Goldman RF.** Physiological responses of men and women to humid and dry heat. *J Appl Physiol Respir Environ Exerc Physiol* 49: 1–8, 1980. doi:10.1152/jappl.1980.49.1.1.
37. **Buller MJ, Welles AP, Friedl KE.** Wearable physiological monitoring for human thermal-work strain optimization. *J Appl Physiol* 124: 432–441, 2018. doi:10.1152/japplphysiol.00353.2017.
38. **Wang F.** Rethinking the core temperature inflection method: misjudging thresholds of human adaptability to extreme heat. *Am J Physiol Regul Integr Comp Physiol* 329: R150–R151, 2025. doi:10.1152/ajpregu.00021.2025.
39. **Schlader ZJ, Johnson BD, Pryor RR, Stooks J, Clemency BM, Hostler D.** Human thermoregulation during prolonged exposure to warm and extremely humid environments expected to occur in disabled submarine scenarios. *Am J Physiol Regul Integr Comp Physiol* 318: R950–R960, 2020. doi:10.1152/ajpregu.00018.2020.
40. **Shoenfeld Y, Udassin R, Shapiro Y, Ohri A, Sohar E.** Age and sex difference in response to short exposure to extreme dry heat. *J Appl Physiol Respir Environ Exerc Physiol* 44: 1–4, 1978. doi:10.1152/jappl.1978.44.1.1.
41. **Kenney WL, Munce TA.** Invited review: aging and human temperature regulation. *J Appl Physiol* 95: 2598–2603, 2003. doi:10.1152/japplphysiol.00202.2003.

Figure captions

Figure 1 Schematic illustration of the two humidity ramp protocols. **A**, *Aggressive-ramp*: an initial 30-min stabilization at 42 °C, followed by 2% RH increments every 5 min until 88% RH (total exposure duration = 180 min); **B**, *Slow-ramp*: an initial 4-hour stabilization at 42 °C and 40% RH, followed by 6% RH increments per hour for 2 hours (to 52% RH), and then 3% RH increments per hour for up to 3 hours (to 61% RH; total exposure duration = 9 hours). The programmed set values (blue lines) and the observed mean wet-bulb temperature (T_w) with standard deviation (tan line with pink band) are shown for each protocol. Note: all T_w values reported in the present study are calculated using the Stull equation (25).

Figure 2 Critical wet-bulb temperatures ($T_{w,critical}$) thresholds determined using aggressive- and slow-ramp humidity protocols at a constant dry-bulb temperature of 42 °C in males (n=14; **Panels A** and **B**) and females (n=12; Panels **C** and **D**). Panels **A** and **C** show scatter plots comparing $T_{w,critical}$ values obtained from the aggressive-ramp (Δt = 5 min) and slow-ramp (Δt = 60 min) protocols for each participant. The grey dotted line represents the line of identity ($y = x$). All data points lie above this line, indicating systematically lower $T_{w,critical}$ values with the aggressive-ramp protocol in both sexes. These systematic underestimations likely arise from the shorter ramp duration (2% RH increase per 5 min), which induces a premature inflection point compared with the slower protocol (60 min per 6%/3% increase). Panels **B** and **D** display paired matchstick plots, with each line connecting the same participant's $T_{w,critical}$ values from both conditions. All lines slope upward, confirming higher critical limits with the slow-ramp protocol. The narrower distribution of slow-ramp values indicates lower inter-individual variability and greater measurement consistency, whereas the wider spread in aggressive-ramp values reflects higher inter-individual variability under rapid humidity increments in both sexes.

Figure 3 Time course (τ) of rectal temperature (T_{cr}) re-stabilization under the adaptive ramp protocol in six representative male (**A–F**) and three female (**G–I**) participants at T_{db}=42 °C, following initial equilibration at 38% RH. Stepwise relative humidity (RH) increments of 3%, 6%, or 10% were applied only after prior T_{cr} stabilization (defined as $|dT_{cr}/dt| \leq 0.1$ °C over 30 min). Green and pink shaded areas denote the 30-min stabilization periods in males and females, respectively. Total exposure durations ranged from 8–10 h (480–600 min). Circles with a grey border and pink fill mark the identified inflection points. No inflection was observed in panel **A** throughout the entire 570 min. Inflection points in panels **B–I** occurred at 33.4 °C (447 min), 33.7 °C (476 min), 33.5 °C (319 min),

34.0 °C (536 min), 33.5 °C (392 min), 33.8 °C (465 min), 34.5 °C (409 min), and 34.3 °C (520 min), respectively.

Figure 4 Time course of rectal temperature (T_{cr}) responses and ambient wet-bulb temperature (T_w) during prolonged stable exposures at T_{db}=42 °C in males and females. A, T_{cr} in males at target T_w=32.7 °C (compensable) and T_w=34.3 °C (uncompensable); B, corresponding measured T_w in the heat chamber for males; C, T_{cr} in females at target T_w=33.1 °C (compensable) and T_w=34.6 °C (uncompensable); D, corresponding measured T_w in the heat chamber for males; Data are means ± SD; compensability defined as T_{cr} stabilization (< 0.10 °C/h slope after 3 h, maintained ≥20 min), uncompensability as sustained T_{cr} rise (> 0.10 °C/h without plateau).

Tables

Table 1 Sensitivity analysis of the dynamic response to step duration (Δt) relative to the physiological time constant (τ).

Step duration (Δt, min)	**Physiological time constant (τ, min)**			**Predictive response characteristic**	**Artifact risk**
	120	**180**	**240**		
5	0.04	0.03	0.021	Rapid environmental progression; core temperature lags markedly	High
10	0.08	0.06	0.042	Core temperature lags markedly; transient accumulation between steps	High to moderate
60	0.5	0.33	0.25	Partial or near equilibration for faster responders; moderate residual lag; slower for large τ	Low
120	1.0	0.67	0.50	Substantial or full equilibration across steps; minimal residual error	Very low

Note: Artifact risk is categorized into four levels: **High** (substantial accumulation of lag between steps), **Moderate** (moderate lag with transient accumulation), **Low** (minimal lag and near steady-state equilibration), and **Very low** (no significant artifacts; full equilibration); The key determinant of dynamic distortion is the dimensionless ratio $\Delta t/\tau$, where Δt represents the dwell duration and τ the physiological time constant of core temperature equilibration. Smaller values of this ratio indicate more rapid environmental progression relative to the body's thermal response. When $\Delta t/\tau \ll 1$ (e.g., 0.01–0.20), the environment changes faster than the thermoregulatory system can respond, leading to accumulated lag and an apparent early inflection in T_{cr}. When $\Delta t/\tau \approx 1$, full equilibration occurs and transient effects are greatly reduced. When $\Delta t/\tau >$ 0.3–0.5, the response effectively reaches near quasi-steady state, and dynamic lags and associated artifacts are largely eliminated.

Figure 1

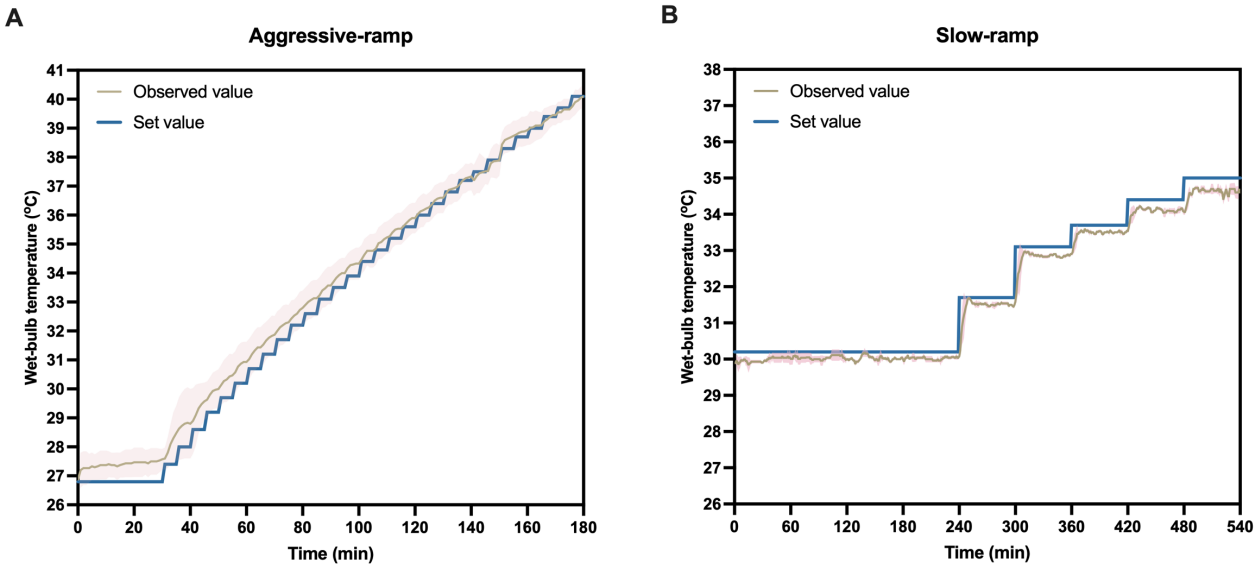
A
Aggressive-ramp
Observed value
Set value
Wet-bulb temperature (°C)
Time (min)
B
Slow-ramp
Observed value
Set value
Wet-bulb temperature (°C)
Time (min)

Figure 2

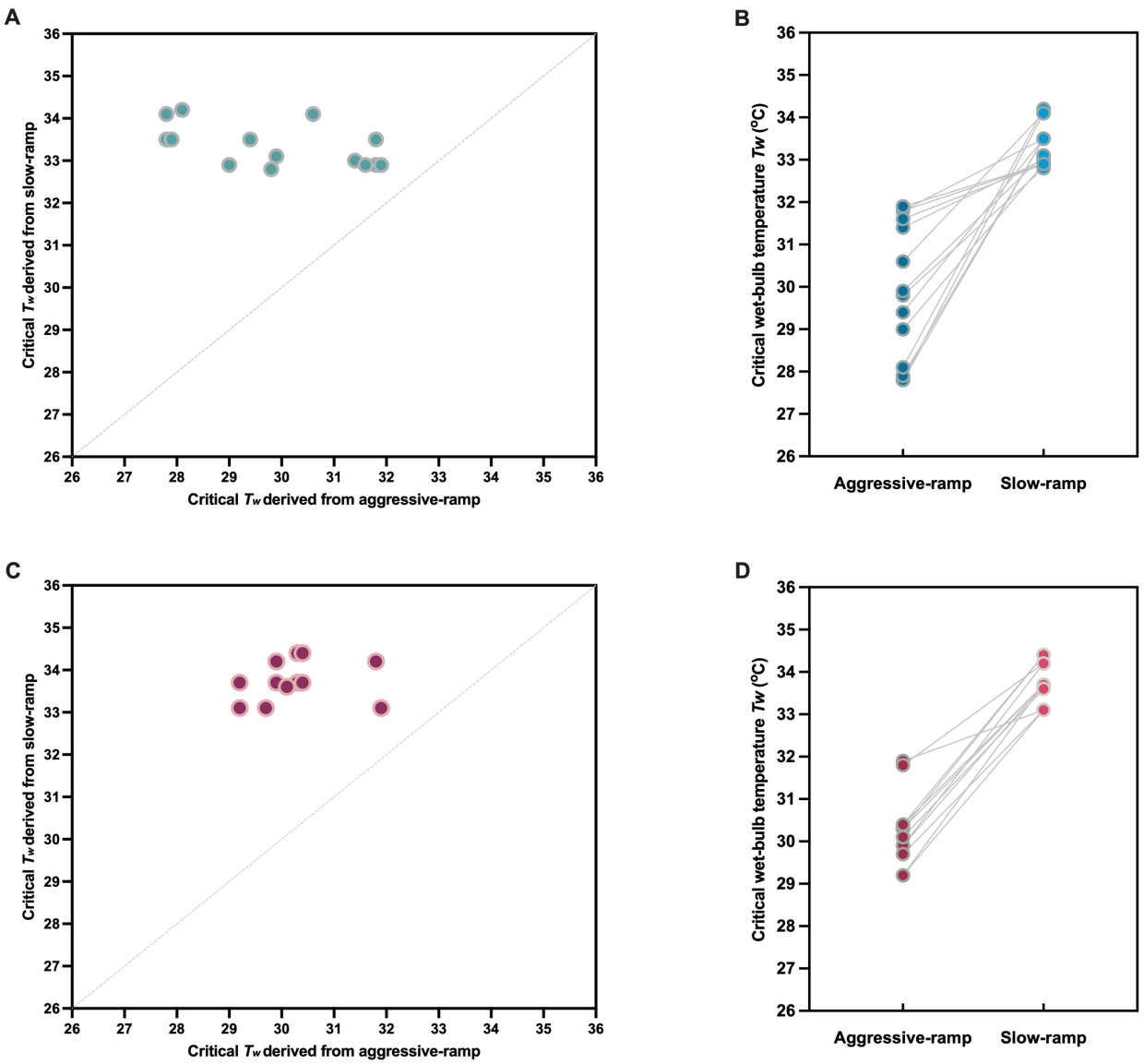
A
Critical T_w derived from slow-ramp
Critical T_w derived from aggressive-ramp
B
Critical wet-bulb temperature T_w (°C)
Aggressive-ramp
Slow-ramp
C
Critical T_w derived from slow-ramp
Critical T_w derived from aggressive-ramp
D
Critical wet-bulb temperature T_w (°C)
Aggressive-ramp
Slow-ramp

Figure 3

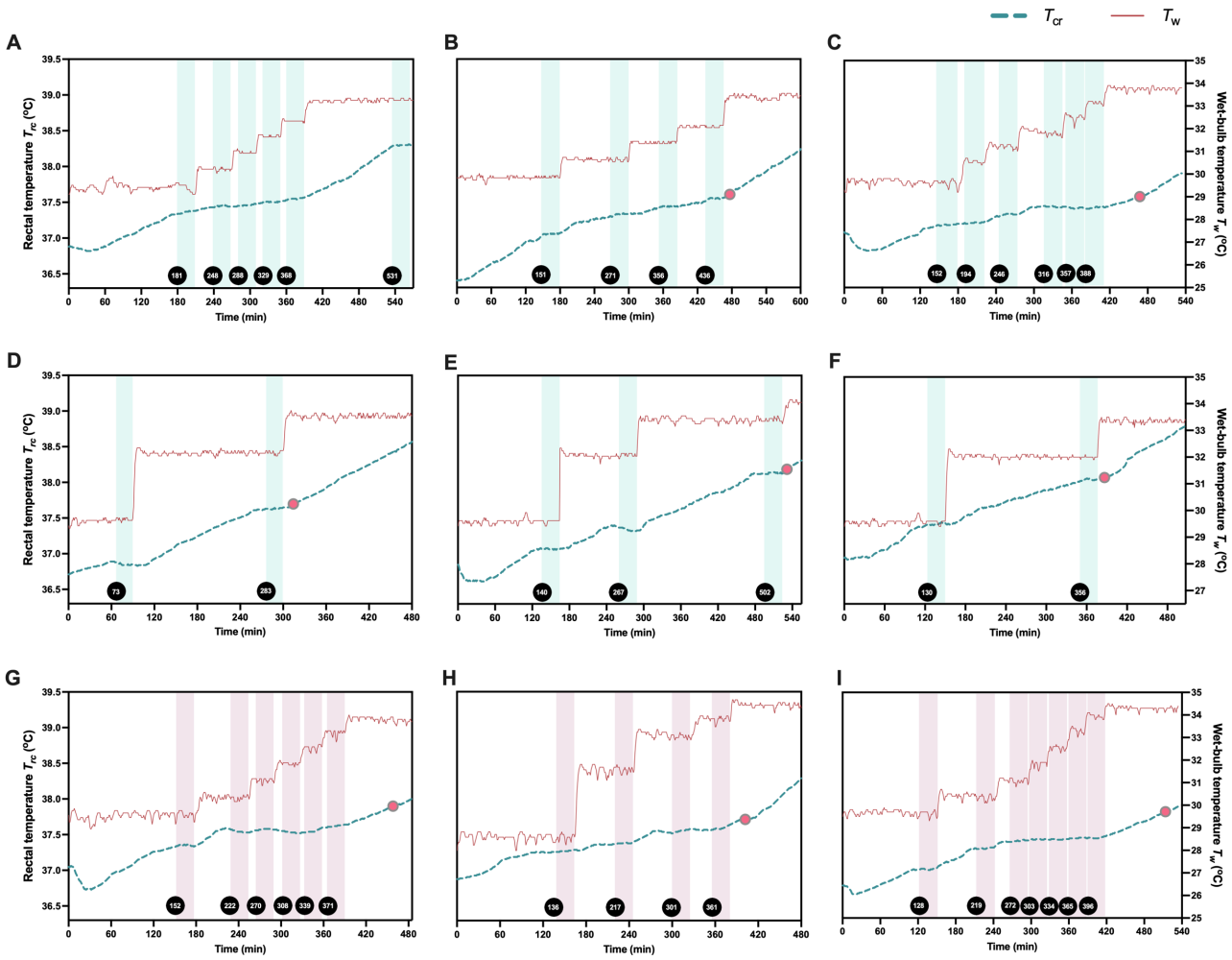
T_{cr}
T_w
A
B
C
D
E
F
G
H
I
Rectal temperature T_{rc} (°C)
Wet-bulb temperature T_w (°C)
Time (min)

Figure 4

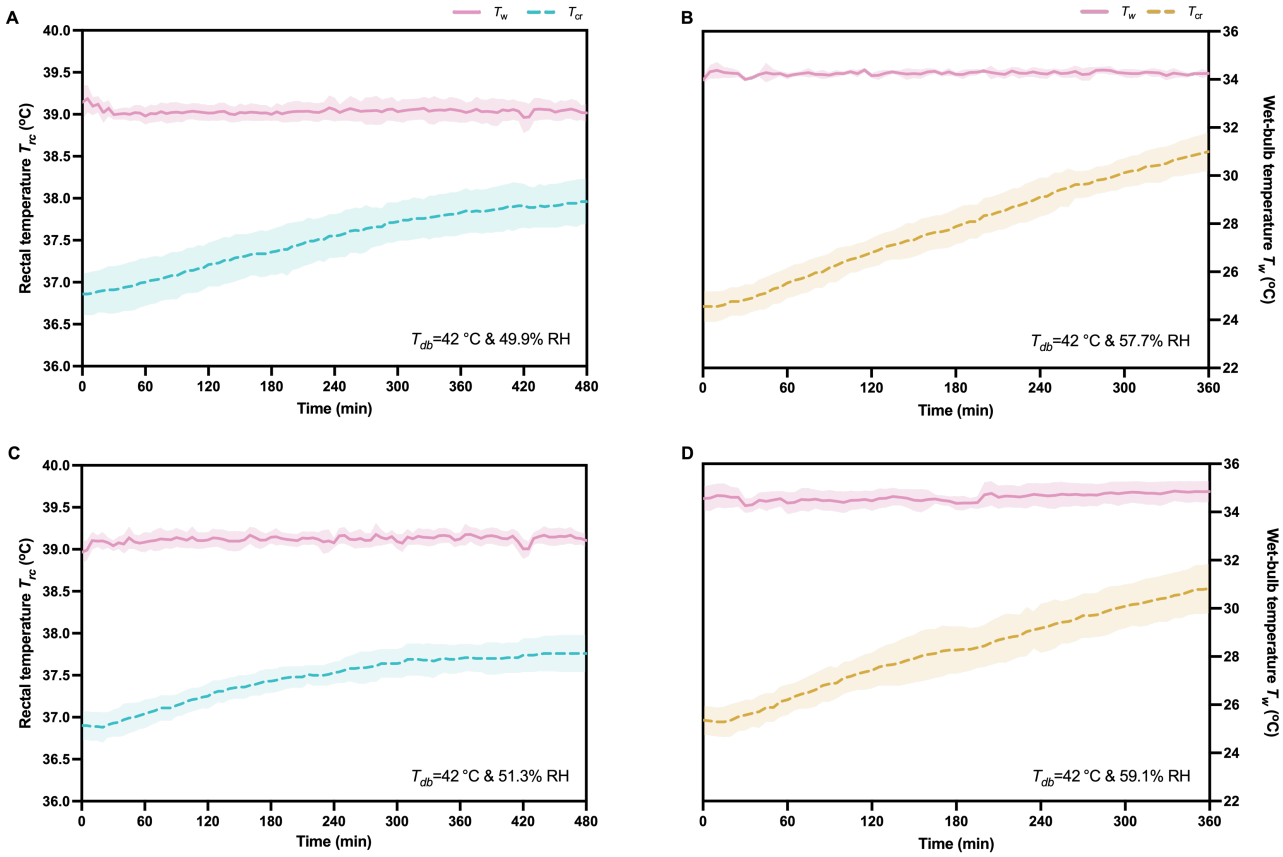
A
B
C
D
T_w
T_{cr}
Rectal temperature T_{rc} (°C)
Wet-bulb temperature T_w (°C)
Time (min)
T_{db}=42 °C & 49.9% RH
T_{db}=42 °C & 57.7% RH
T_{db}=42 °C & 51.3% RH
T_{db}=42 °C & 59.1% RH